www.sciencemag.org/content/358/6364/781/suppl/DC1

Supplementary Materials for

Cordilleran Ice Sheet mass loss preceded climate reversals near the Pleistocene Termination

B. Menounos,* B. M. Goehring, G. Osborn, M. Margold, B. Ward, J. Bond, G. K. C. Clarke, J. J. Clague, T. Lakeman, J. Koch, M. W. Caffee, J. Gosse, A. P. Stroeven, J. Seguinot, J. Heyman

*Corresponding author. Email: menounos@unbc.ca

Published 10 November 2017, *Science* **358**, 781 (2017)
DOI: 10.1126/science.aan3001

This PDF file includes:

Other Supplementary Material for this manuscript includes the following:
(available at www.sciencemag.org/cgi/content/full/358/6364/781/DC1)

Data S1 (Excel file)
Site and sample characteristics and chemical, analytical data, and age data

Data S2 (Excel file)
Numerical ages used in this study other than new exposure ages

Data S3 (Excel file)
Estimated ELA and temperature depression for moraines of this study

Data S4 (KMZ file)
Sample locations, characteristics, and images. Additional Late Pleistocene moraines. Data contained in Google Earth KMZ file.

Materials and Methods

We identified moraines using aerial photographs, satellite imagery, and field reconnaissance. Helicopter support was required to reach remote moraines; both weight and time constraints limited the number of boulders that we could sample at each site. We sampled large boulders in stable positions on outermost moraines for ^{10}Be analysis. At two sites we collected a single sample, as there were no other suitable boulders. Sites were located using hand-held global positioning system (GPS) units, and elevations were determined from the GPS or using a barometric altimeter (±10 m). We determined shielding of cosmic rays by the surrounding topography and by the boulders themselves using an inclinometer and compass. Samples were physically and chemically prepared at the Purdue Rare Isotope Measurement (PRIME) Laboratory, the Lamont Doherty Earth Observatory Cosmogenic Nuclide Laboratory (LDEO), the Tulane University Cosmogenic Nuclide Laboratory (TUCNL), and the Dalhousie University Terrestrial Cosmogenic Nuclide Exposure Facility (DAL). These laboratories employ standard physical and chemical preparation procedures for terrestrial nuclide samples. Beryllium-isotope ratio analyses were performed at PRIME Laboratory (n=58) and the Lawrence Livermore National Laboratory Center for Accelerator Mass Spectrometry (n=18) relative to the ^{10}Be/^{9}Be standard 07KNSTD (*31*).

We calculated ^{10}Be exposure ages using code based on the web calculator at http://www.hess.ess.washington.edu. The scaling model (*32*) uses a recent ^{10}Be production rate (*33*) for a global dataset; no corrections were made for snow cover or surface erosion. Uncertainties on reported exposure ages represent analytical uncertainty only.

Surface Exposure Sample Preparation and Age Determination

Samples were first crushed, milled, and sieved to isolate the 250-500 or 125-750 micron size fraction. Quartz was isolated using froth flotation of feldspar and other mineral phases, magnetic mineral separation, heavy liquid mineral separation, and successive weak HF/HNO_3 acid leaches to both isolate quartz and etch quartz grain surfaces to remove meteoric ^{10}Be (*34*).

Pure quartz aliquots were spiked with a known quantity (~0.2 – 0.3 mg Be) of low-level beryllium carrier (^{10}Be/^{9}Be ratio < $5e^{-15}$) and then dissolved in a 5:1 mixture of HF and HNO_3. Beryllium was isolated using a combination of pH precipitations and cation chromatography (PRIME), or in successive anion and cation chromatography columns (LDEO, DAL, and TUCNL). The beryllium fraction was precipitated as a $BeOH_2$ gel and calcined at 1000°C to form BeO. The BeO was powdered, mixed with niobium powder, and packed into targets for accelerator mass spectrometry measurement.

Beryllium-isotope ratio analyses were performed at PRIME (n=58) and the Lawrence Livermore National Laboratory Center for Accelerator Mass Spectrometry (LLNL-CAMS, n=18) relative to the ^{10}Be/^{9}Be standard (*31*) 07KNSTD. Isotope ratios were converted to the total number of ^{10}Be atoms in the sample or process blank. Each sample was then corrected for the background ^{10}Be level by subtracting the number of ^{10}Be atoms in the respective process blank from the set of samples associated with the process blank. Sample concentrations were calculated by normalizing the total number of ^{10}Be atoms in the sample by the mass of quartz dissolved. All errors associated with

measurement and background correction are propagated in quadrature (*35*). Analytical results (Additional Data Table S1) follow minimum reporting requirements for ^{10}Be studies (*36*).

Ages presented in the main body of the paper are minimum exposure ages. For completeness, we also present in Data Table S1 exposure ages adjusted for possible erosion and snow cover, as well as a combination of the two; these are considered to be maximum age estimates. Snow shielding correction factors are derived from the British Columbia River Forecast Center's network of automated snow weather stations (i.e., Snowpillow; http://bcrfc.env.gov.bc.ca/data/asp/). For each sample, we include the average annual shielding correction based on reported snow-water equivalent (SWE) depths and the station ID.

An exposure age can also potentially be corrected for glacial isostatic rebound. However, given our approach to use minimum exposure ages in this study, we do not incorporate corrections for isostatic rebound. Any possible correction is also complicated by unquantifiable corrections for atmospheric pressure (*37*). Using four characteristic locations (sites 2, 7, 15, and 23), we extract elevation histories from the ICE-6G reconstruction (*38*) to determine elevation histories for these sites. The magnitude of correction for an exposure age that underwent isostatic rebound is primarily dependent on the magnitude and duration of depression. For sites in the Canadian Cordillera, the depression magnitude can be large, but it is relatively short-lived after 14 ka. As such, average isostatic rebound corrections for the above sites are 11.8%, 11.3%, 10.4%, and 10% (Fig. S1).

Uncertainties on reported exposure ages represent analytical uncertainty only. The summary age for a site is generated using the median and interquartile range of all samples, including possible outliers. We argue that this approach is conservative, as the median will be most strongly affected by samples clustering together and thus provides a robust moraine age while accounting for the observed scatter at a site using the interquartile range and is independent of absolute measurement uncertainties.

Exposure ages were calculated using computer code (http://hess.ess.washington.edu) modified for use with a scaling model (*31*) that employs an atmospheric sea-level air pressure model derived from the ERA40 Reanalysis (*38*). No corrections were made for changes in sample elevation due to isostatic rebound. All ages presented in the text and figures were generated using the zero erosion exposure age (Additional Data Table S1).

At present there is no regional ^{10}Be production rate calibration site for British Columbia or the Yukon. We thus used the global compilation of production rates (*33*) as part of the CRONUS-Earth effort (P ^{10}Be = 4.00±0.38 atoms g^{-1} yr^{-1}). Use of ^{10}Be calibration sites from high latitudes (*39*) in the Northern Hemisphere yields equivalent results. The use of a global dataset removes any ambiguities that might arise in choosing what defines a local production rate in space and time, as well as its applicability to sites of unknown ages. We note that the reference rates in the Northern Hemisphere study predate the scaling model described above. We updated the calibrated production rates to incorporate the scaling and atmospheric models of Lifton to yield a sea-level, high-latitude ^{10}Be production rate of 4.05±0.14 atoms g^{-1} yr^{-1}.

Supplementary Text

Families of Moraines

Although marginal retreat was common during the demise of the CIS, especially in areas of more subdued topography (*40*), few moraines exist that record ice sheet retreat in areas of high relief. In contrast, many alpine moraines occur throughout the region's many mountain ranges.

Most outermost valley and cirque moraines in western Canada were constructed about 170-320 years ago during the Little Ice Age (LIA) (*41*). In some ranges, however, one or two moraines lie beyond the LIA glacial limit and, unlike their LIA counterparts, are more subdued and commonly vegetated, indicating their relative antiquity compared to the LIA. Based on previous work (*6*) that mapped the extent of the CIS during the Last Glacial Maximum (18 ka) these pre LIA moraines formed following decay of the CIS (Figs. S2 and S3).

One set of pre-LIA moraines lies within high-elevation cirques and extends only tens to hundreds of meters beyond the LIA limit. We refer to these features as 'cirque moraines'. In general, the cirque moraines are low looping ridges with subdued crests that have not been breached by stream erosion. Such moraines in the Canadian Cordillera were first described (*42*) as products of the "Crowfoot Advance" and initially were only known to be older than about 7700 years. Dating of lake sediments interpreted to be associated with the type Crowfoot moraine led to a presumed YD age for the advance (*10*). The moraines lie just outside Little Ice Age (LIA) end moraines or, in some instances, are partly overlain by LIA moraines. In most cirques in the Canadian Rockies there are no Crowfoot-type moraines, suggesting that either the LIA advance was more extensive than the Crowfoot Advance or that these cirques were beneath the Cordilleran Ice Sheet.

Representative examples of high-elevation cirque moraines in this study are the Fried Egg, Birkenhead, and Diamond moraines, which are approximately 70 m, 225 m, and 190 m, respectively, beyond Little Ice Age maximum extents (sites 2-4 of Fig. 1, Additional Data Table S1, and Supplementary Data File S4). These moraines and the other cirque moraines examined in this study are at high elevations where seasonal snow cover is potentially an issue for cosmogenic dating.

Another set, found only within some ranges, consists of lateral and end moraines that extend down large valleys and terminate many kilometers beyond LIA deposits. We refer to these features as 'valley moraines'. The valley moraines are only found within some ranges and consists of lateral and end moraines that extend down large valleys and terminate many kilometers beyond LIA limits. Most of the large valley moraines were built by classic alpine valley glaciers, but some show geomorphic evidence of having terminated on or adjacent to stagnating ice in adjacent trunk valleys (*43*).

Although pre-LIA cirque and valley moraines exist throughout the Canadian Cordillera, most of them occur in intermediate to high-elevation, leeward locations in the Coast, Cassiar, and St. Elias mountains (Fig. 1), far from what would have been the outer margins of the CIS. There are concentrations of valley moraines in the Finlay River area in the Omineca Mountains, the headwaters of Homathko River on the east flank of the Coast Mountains, the Skeena Mountains east of Dease Lake, the Nahanni River watershed in Northwest Territories, and on Level Mountain northwest of Dease Lake (*43*). The valley moraines in the Finlay River area, which are described in detail

elsewhere (*43*), are sharp-crested, up to 120 m high, and extend as far as 9 km beyond Little Ice Age limits. Several lateral moraines are cross-cut by meltwater channels that record down-wasting of trunk valley ice of the northern CIS, whereas other moraines merge with ice-stagnation deposits in trunk valleys. These relationships demonstrate that advancing alpine glaciers interacted with the decaying CIS.

Temperature ELA Reconstruction Estimates

To provide first-order estimates of the average temperatures responsible for the valley and cirque moraines of this study, we examined changes in the equilibrium line altitudes (ELA) for LIA and latest Pleistocene glaciers in the study area. Several methods exist for estimating past ELA (*44*), and we chose the accumulation ablation ratio (AAR) using an accumulation area ratio of 0.6 for contemporary, LIA, and latest Pleistocene glacier extents. The absolute magnitude of ELA-based temperature estimates varies among reconstruction methods (44), but our intention here is to illustrate the relative differences in reconstructed temperatures between moraine groups.

Using Google Earth, we selected ten sites throughout the Coast Mountains (Additional Data Table S3 and Additional Data File S4) that contained contemporary ice, and moraines of LIA and latest Pleistocene age. From the mapped ice extents, we generated hypsometric curves for each paleo-glacier and calculated depressions of the ELA from present day. We use a thermal lapse rate of -6.5 °C km^{-1} to convert changes in ELA position to temperature change.

Others have used glacier extent as a climate proxy (45), but this is potentially problematic because in the CIS region contemporaneous moraines have differing downvalley extent. Simple climate reconstructions using equilibrium line depressions and standard lapse rates (Table S3) indicate that cooling of 2.51 ± 0.41°C (SEM) relative to today would be required to construct the valley moraines if the advances were primarily driven by temperature change, whereas the cirque moraines could be built with a temperature depression of 0.57 ± 0.22°C. These temperature differences are implausible because age-equivalent valley and cirque moraines are near one another and thus rule out forcing by regional climate variability.

Previously published numerical ages

Please refer to Additional Data Table S2 for other numerical ages used in our study.

Supplementary Figure S1

Isostatic depression relative to modern elevations for grid cells encompassing four characteristic locations in our study. Depression amounts are derived from ICE-6G model (*8*).

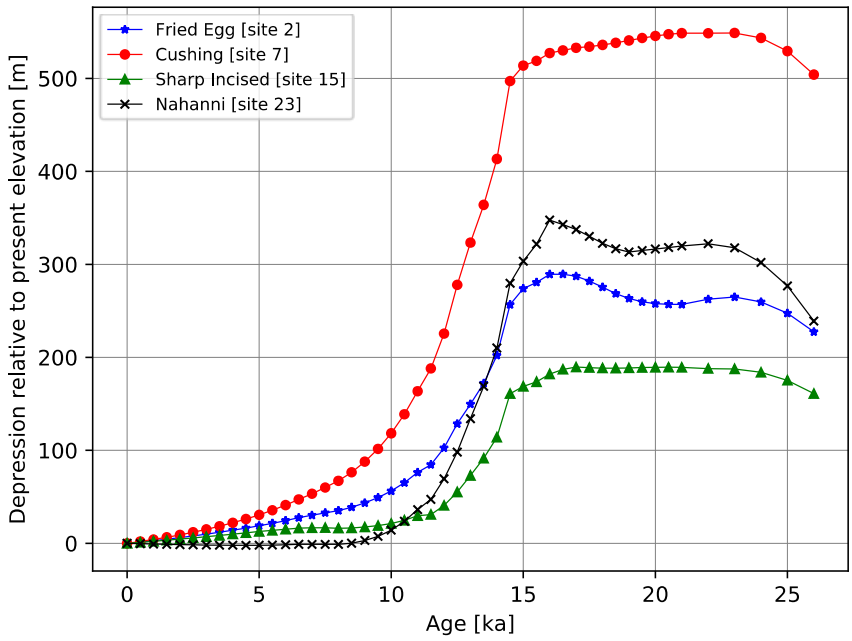

Supplementary Figure S2

(A) Configuration of the CIS (*76*) at about 18 ka. Deglaciation ages (^{10}Be) and locations of valley glaciers that advanced after regional ice sheet deglaciation are drawn with the same color scheme as in Fig. 1. (B) Close-up of CIS down wasting in the Whitehorse area. Sample 11JB28 MM1 at 1377 m above sea level, dated to 14.8 ka, marks the time when the ice sheet surface dropped below the elevation of the low ridges surrounding the Yukon River valley. Although higher summits in the area emerged above the ice sheet surface even earlier, the valley bottom only became ice free at about 13 ka, immediately before the YD.

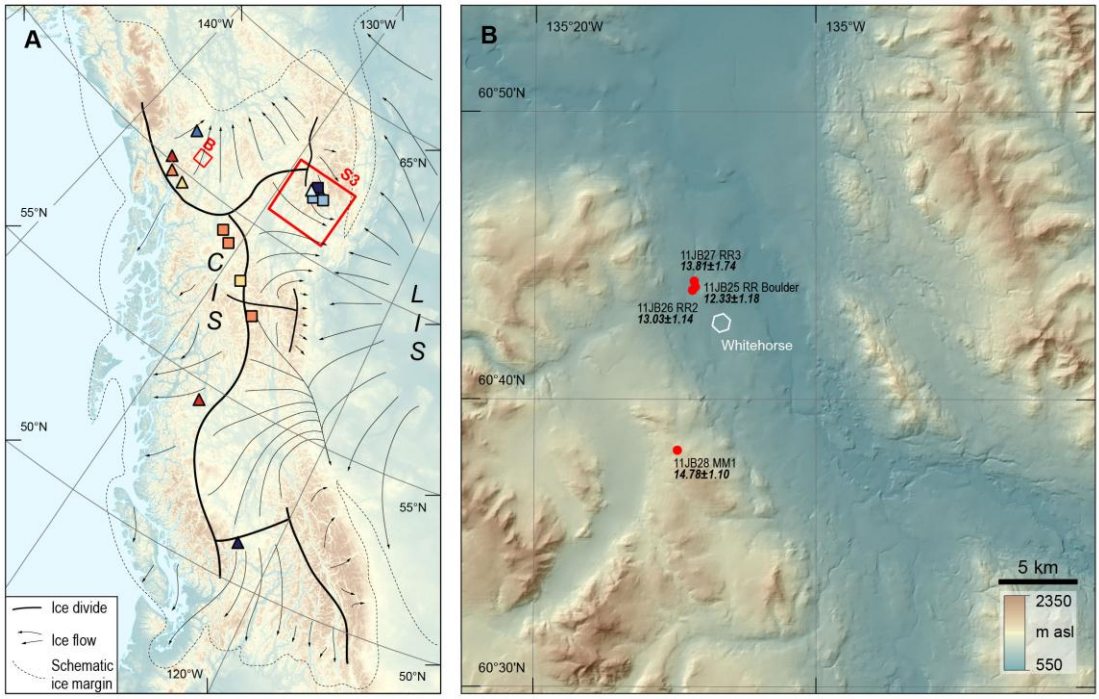

Supplementary Figure S3

Configuration of the Liard lobe of the CIS at the LGM showing inundation of valley moraines (sites 23-25 and r in Fig. 1) that were deglaciated during the latest Pleistocene. Dated moraines head from cirques, and their orientations are inconsistent with the ice-flow configuration at the CIS maximum. Their ages can thus be used to provide a minimum-limiting age for CIS deglaciation at these locations.

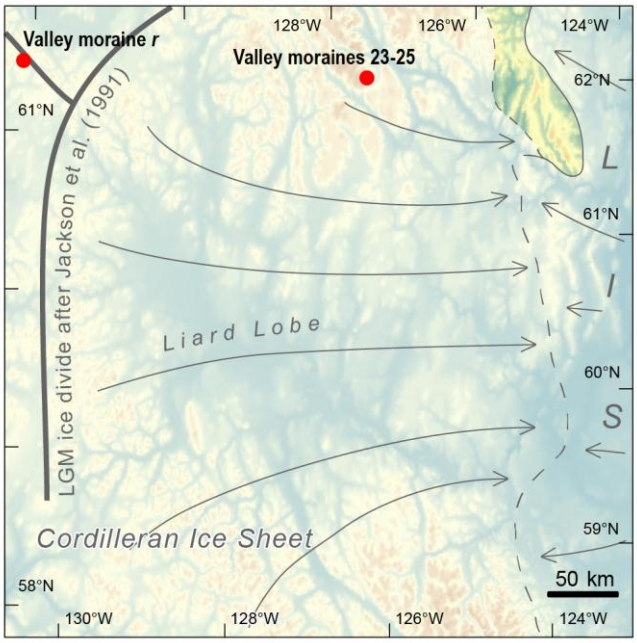

Additional Data table S1 (separate file)

Site and sample characteristics and chemical, analytical data, and age data.

Additional Data table S2 (separate file)

Numerical ages used in this study other than new exposure ages.

Additional Data table S3 (separate file)

Estimated ELA and temperature depression for moraines of this study

Additional Data S4 (separate file)

Sample locations, characteristics, and images. Additional Late Pleistocene moraines. Data contained in Google Earth KMZ file.

References

1. P. U. Clark, J. D. Shakun, P. A. Baker, P. J. Bartlein, S. Brewer, E. Brook, A. E. Carlson, H. Cheng, D. S. Kaufman, Z. Liu, T. M. Marchitto, A. C. Mix, C. Morrill, B. L. Otto-Bliesner, K. Pahnke, J. M. Russell, C. Whitlock, J. F. Adkins, J. L. Blois, J. Clark, S. M. Colman, W. B. Curry, B. P. Flower, F. He, T. C. Johnson, J. Lynch-Stieglitz, V. Markgraf, J. McManus, J. X. Mitrovica, P. I. Moreno, J. W. Williams, Global climate evolution during the last deglaciation. *Proc. Natl. Acad. Sci. U.S.A.* **109**, E1134–E1142 (2012). doi:10.1073/pnas.1116619109 Medline

2. P. Deschamps, N. Durand, E. Bard, B. Hamelin, G. Camoin, A. L. Thomas, G. M. Henderson, J. Okuno, Y. Yokoyama, Ice-sheet collapse and sea-level rise at the Bølling warming 14,600 years ago. *Nature* **483**, 559–564 (2012). doi:10.1038/nature10902 Medline

3. S. O. Rasmussen, M. Bigler, S. P. Blockley, T. Blunier, S. L. Buchardt, H. B. Clausen, I. Cvijanovic, D. Dahl-Jensen, S. J. Johnsen, H. Fischer, V. Gkinis, M. Guillevic, W. Z. Hoek, J. J. Lowe, J. B. Pedro, T. Popp, I. K. Seierstad, J. P. Steffensen, A. M. Svensson, P. Vallelonga, B. M. Vinther, M. J. C. Walker, J. J. Wheatley, M. Winstrup, A stratigraphic framework for abrupt climatic changes during the Last Glacial period based on three synchronized Greenland ice-core records: Refining and extending the INTIMATE event stratigraphy. *Quat. Sci. Rev.* **106**, 14–28 (2014). doi:10.1016/j.quascirev.2014.09.007

4. S. K. Praetorius, A. C. Mix, Synchronization of North Pacific and Greenland climates preceded abrupt deglacial warming. *Science* **345**, 444–448 (2014). doi:10.1126/science.1252000 Medline

5. J. Seguinot, I. Rogozhina, A. P. Stroeven, M. Margold, J. Kleman, Numerical simulations of the Cordilleran ice sheet through the last glacial cycle. *Cryosphere* **10**, 639–664 (2016). doi:10.5194/tc-10-639-2016

6. A. S. Dyke, in *Developments in Quaternary Science*, J. Ehlers, P. L. Gibbard, Eds. (Elsevier, 2004), vol. 2, pp. 373–424.

7. L. Tarasov, A. S. Dyke, R. M. Neal, W. R. Peltier, A data-calibrated distribution of deglacial chronologies for the North American ice complex from glaciological modeling. *Earth Planet. Sci. Lett.* **315–316**, 30–40 (2012). doi:10.1016/j.epsl.2011.09.010

8. W. R. Peltier, D. F. Argus, R. Drummond, Space geodesy constrains ice age terminal deglaciation: The global ICE-6G_C (VM5a) model. *J. Geophys. Res. Solid Earth* **120**, 450–487 (2015). doi:10.1002/2014JB011176

9. A. D. Wickert, Reconstruction of North American drainage basins and river discharge since the Last Glacial Maximum. *Earth Surf. Dyn.* **4**, 831–869 (2016). doi:10.5194/esurf-4-831-2016

10. M. A. Reasoner, G. Osborn, N. W. Rutter, Age of the Crowfoot advance in the Canadian Rocky Mountains: A glacial event coeval with the Younger Dryas oscillation. *Geology* **22**, 439–442 (1994). doi:10.1130/0091-7613(1994)022<0439:AOTCAI>2.3.CO;2

11. P. Friele, J. J. Clague, Younger Dryas readvance in Squamish river valley, southern Coast mountains, British Columbia. *Quat. Sci. Rev.* **21**, 1925–1933 (2002). doi:10.1016/S0277-3791(02)00081-1

12. D. J. Kovanen, Morphologic and stratigraphic evidence for Allerød and Younger Dryas age glacier fluctuations of the Cordilleran Ice Sheet, British Columbia, Canada and Northwest Washington, U.S.A. *Boreas* **31**, 163–184 (2002). doi:10.1080/030094802320129962

13. J. B. R. Eamer, D. H. Shugar, I. J. Walker, O. B. Lian, C. M. Neudorf, A. M. Telka, A glacial readvance during retreat of the Cordilleran Ice Sheet, British Columbia central coast. *Quat. Res.* **87**, 468–481 (2017). doi:10.1017/qua.2017.16

14. R. W. Mathewes, L. E. Heusser, R. T. Patterson, Evidence for a Younger Dryas-like cooling event on the British Columbia coast. *Geology* **21**, 101–104 (1993). doi:10.1130/0091-7613(1993)021<0101:EFAYDL>2.3.CO;2

15. M. A. Taylor, I. L. Hendy, D. K. Pak, Deglacial ocean warming and marine margin retreat of the Cordilleran Ice Sheet in the North Pacific Ocean. *Earth Planet. Sci. Lett.* **403**, 89–98 (2014). doi:10.1016/j.epsl.2014.06.026

16. J. M. Lora, J. L. Mitchell, A. E. Tripati, Abrupt reorganization of North Pacific and western North American climate during the last deglaciation. *Geophys. Res. Lett.* **43**, 11,796–11,804 (2016). doi:10.1002/2016GL071244

17. P. D. Heintzman, D. Froese, J. W. Ives, A. E. R. Soares, G. D. Zazula, B. Letts, T. D. Andrews, J. C. Driver, E. Hall, P. G. Hare, C. N. Jass, G. MacKay, J. R. Southon, M. Stiller, R. Woywitka, M. A. Suchard, B. Shapiro, Bison phylogeography constrains dispersal and viability of the Ice Free Corridor in western Canada. *Proc. Natl. Acad. Sci. U.S.A.* **113**, 8057–8063 (2016). doi:10.1073/pnas.1601077113 Medline

18. B. Llamas, L. Fehren-Schmitz, G. Valverde, J. Soubrier, S. Mallick, N. Rohland, S. Nordenfelt, C. Valdiosera, S. M. Richards, A. Rohrlach, M. I. B. Romero, I. F. Espinoza, E. T. Cagigao, L. W. Jiménez, K. Makowski, I. S. L. Reyna, J. M. Lory, J. A. B. Torrez, M. A. Rivera, R. L. Burger, M. C. Ceruti, J. Reinhard, R. S. Wells, G. Politis, C. M. Santoro, V. G. Standen, C. Smith, D. Reich, S. Y. W. Ho, A. Cooper, W. Haak, Ancient mitochondrial DNA provides high-resolution time scale of the peopling of the Americas. *Sci. Adv.* **2**, e1501385 (2016). doi:10.1126/sciadv.1501385 Medline

19. L. J. Gregoire, B. Otto-Bliesner, P. J. Valdes, R. Ivanovic, Abrupt Bølling warming and ice saddle collapse contributions to the meltwater pulse 1a rapid sea level rise. *Geophys. Res. Lett.* **43**, 9130–9137 (2016). doi:10.1002/2016GL070356 Medline

20. R. F. Ivanovic, L. J. Gregoire, A. D. Wickert, P. J. Valdes, A. Burke, Collapse of the North American ice saddle 14,500 years ago caused widespread cooling and reduced ocean overturning circulation. *Geophys. Res. Lett.* **44**, 383–392 (2017). doi:10.1002/2016GL071849

21. K. Lambeck, A. Purcell, S. Zhao, The North American Late Wisconsin ice sheet and mantle viscosity from glacial rebound analyses. *Quat. Sci. Rev.* **158**, 172–210 (2017). doi:10.1016/j.quascirev.2016.11.033

22. Z. Liu, B. L. Otto-Bliesner, F. He, E. C. Brady, R. Tomas, P. U. Clark, A. E. Carlson, J. Lynch-Stieglitz, W. Curry, E. Brook, D. Erickson, R. Jacob, J. Kutzbach, J. Cheng, Transient simulation of last deglaciation with a new mechanism for Bolling-Allerod warming. *Science* **325**, 310–314 (2009). doi:10.1126/science.1171041 Medline

23. W. R. Peltier, Global glacial isostacy and the surface of the ice-age Earth: The ICE-5G (VM2) model and GRACE. *Annu. Rev. Earth Planet. Sci.* **32**, 111–149 (2004). doi:10.1146/annurev.earth.32.082503.144359

24. S. K. Praetorius, A. C. Mix, M. H. Walczak, M. D. Wolhowe, J. A. Addison, F. G. Prahl, North Pacific deglacial hypoxic events linked to abrupt ocean warming. *Nature* **527**, 362–366 (2015). doi:10.1038/nature15753 Medline

25. M. H. Davies, A. C. Mix, J. S. Stoner, J. A. Addison, J. Jaeger, B. Finney, J. Wiest, The deglacial transition on the southeastern Alaska Margin: Meltwater input, sea level rise, marine productivity, and sedimentary anoxia. *Paleoceanography* **26**, PA2223 (2011). doi:10.1029/2010PA002051

26. A. E. Carlson, What caused the Younger Dryas cold event? *Geology* **38**, 383–384 (2010). doi:10.1130/focus042010.1

27. R. J. Fulton, A conceptual model for growth and decay of the Cordilleran Ice Sheet. *Geogr. Phys. Quat.* **45**, 281 (1991). doi:10.7202/032875ar

28. K. K. Andersen, N. Azuma, J.-M. Barnola, M. Bigler, P. Biscaye, N. Caillon, J. Chappellaz, H. B. Clausen, D. Dahl-Jensen, H. Fischer, J. Flückiger, D. Fritzsche, Y. Fujii, K. Goto-Azuma, K. Grønvold, N. S. Gundestrup, M. Hansson, C. Huber, C. S. Hvidberg, S. J. Johnsen, U. Jonsell, J. Jouzel, S. Kipfstuhl, A. Landais, M. Leuenberger, R. Lorrain, V. Masson-Delmotte, H. Miller, H. Motoyama, H. Narita, T. Popp, S. O. Rasmussen, D. Raynaud, R. Rothlisberger, U. Ruth, D. Samyn, J. Schwander, H. Shoji, M.-L. Siggard-Andersen, J. P. Steffensen, T. Stocker, A. E. Sveinbjörnsdóttir, A. Svensson, M. Takata, J.-L. Tison, T. Thorsteinsson, O. Watanabe, F. Wilhelms, J. W. C. White; North Greenland Ice Core Project members, High-resolution record of Northern Hemisphere climate extending into the last interglacial period. *Nature* **431**, 147–151 (2004). doi:10.1038/nature02805 Medline

29. A. Berger, M. F. Loutre, Insolation values for the climate of the last 10 million years. *Quat. Sci. Rev.* **10**, 297–317 (1991). doi:10.1016/0277-3791(91)90033-Q

30. A. P. Stroeven, D. Fabel, A. T. Codilean, J. Kleman, J. J. Clague, M. Miguens-Rodriguez, S. Xu, Investigating the glacial history of the northern sector of the Cordilleran Ice Sheet with cosmogenic ^{10}Be concentrations in quartz. *Quat. Sci. Rev.* **29**, 3630–3643 (2010). doi:10.1016/j.quascirev.2010.07.010

31. K. Nishiizumi, M. Imamura, M. W. Caffee, J. R. Southon, R. C. Finkel, J. McAninch, Absolute calibration of ^{10}Be AMS standards. *Nucl. Instruments Methods Phys. Res. Sect. B Beam Interact. with Mater. Atoms* **258**, 403–413 (2007). doi:10.1016/j.nimb.2007.01.297

32. N. Lifton, T. Sato, T. J. Dunai, Scaling in situ cosmogenic nuclide production rates using analytical approximations to atmospheric cosmic-ray fluxes. *Earth Planet. Sci. Lett.* **386**, 149–160 (2014). doi:10.1016/j.epsl.2013.10.052

33. B. Borchers, S. Marrero, G. Balco, M. Caffee, B. Goehring, N. Lifton, K. Nishiizumi, F. Phillips, J. Schaefer, J. Stone, Geological calibration of spallation production rates in the CRONUS-Earth project. *Quat. Geochronol.* **31**, 188–198 (2016). doi:10.1016/j.quageo.2015.01.009

34. C. P. Kohl, K. Nishiizumi, Chemical isolation of quartz for measurement of in-situ-produced cosmogenic nuclides. *Geochim. Cosmochim. Acta* **56**, 3583–3587 (1992). doi:10.1016/0016-7037(92)90401-4

35. P. R. Bevington, D. K. Robinson, *Data Reduction and Error Analysis for the Physical Sciences* (McGraw Hill, 2003) http://books.google.com/books?id=JYaZPwAACAAJ, vol. 8.

36. K. L. Frankel, R. C. Finkel, L. A. Owen, Terrestrial cosmogenic nuclide geochronology data reporting standards needed. *Eos (Wash. D.C.)* **91**, 31–32 (2010). doi:10.1029/2010EO040003

37. J. Staiger, J. Gosse, R. Toracinta, B. Oglesby, J. Fastook, J. V. Johnson, Atmospheric scaling of cosmogenic nuclide production: Climate effect. *J. Geophys. Res.* **112**, B02205 (2007). doi:10.1029/2005JB003811

38. D. P. Dee, S. M. Uppala, A. J. Simmons, P. Berrisford, P. Poli, S. Kobayashi, U. Andrae, M. A. Balmaseda, G. Balsamo, P. Bauer, P. Bechtold, A. C. M. Beljaars, L. van de Berg, J. Bidlot, N. Bormann, C. Delsol, R. Dragani, M. Fuentes, A. J. Geer, L. Haimberger, S. B. Healy, H. Hersbach, E. V. Hólm, L. Isaksen, P. Kållberg, M. Köhler, M. Matricardi, A. P. McNally, B. M. Monge-Sanz, J.-J. Morcrette, B.-K. Park, C. Peubey, P. de Rosnay, C. Tavolato, J.-N. Thépaut, F. Vitart, The ERA-Interim reanalysis: Configuration and performance of the data assimilation system. *Q. J. R. Meteorol. Soc.* **137**, 553–597 (2011). doi:10.1002/qj.828

39. N. E. Young, J. M. Schaefer, J. P. Briner, B. M. Goehring, A ^{10}Be production-rate calibration for the Arctic. *J. Quat. Sci.* **28**, 515–526 (2013). doi:10.1002/jqs.2642

40. A. J. Perkins, T. A. Brennand, Refining the pattern and style of Cordilleran Ice Sheet retreat: Palaeogeography, evolution and implications of late glacial ice-dammed lake systems on the southern Fraser Plateau, British Columbia, Canada. *Boreas* **44**, 319–342 (2015). doi:10.1111/bor.12100

41. B. Menounos, G. Osborn, J. J. Clague, B. H. Luckman, Latest Pleistocene and Holocene glacier fluctuations in western Canada. *Quat. Sci. Rev.* **28**, 2049–2074 (2009). doi:10.1016/j.quascirev.2008.10.018

42. B. H. Luckman, G. D. Osborn, Holocene glacier fluctuations in the middle Canadian Rocky Mountains. *Quat. Res.* **11**, 52–77 (1979). doi:10.1016/0033-5894(79)90069-3

43. T. R. Lakeman, J. J. Clague, B. Menounos, Advance of alpine glaciers during final retreat of the Cordilleran ice sheet in the Finlay River area, northern British Columbia, Canada. *Quat. Res.* **69**, 188–200 (2008). doi:10.1016/j.yqres.2008.01.002

44. S. C. Porter, Snowline depression in the tropics during the last glaciation. *Quat. Sci. Rev.* **20**, 1067–1091 (2001). doi:10.1016/S0277-3791(00)00178-5

45. J. Oerlemans, Extracting a climate signal from 169 glacier records. *Science* **308**, 675–677 (2005). doi:10.1126/science.1107046 Medline

46. S. C. Porter, T. W. Swanson, ^{36}Cl dating of the classic Pleistocene glacial record in the northeastern Cascade Range, Washington. *Am. J. Sci.* **308**, 130–166 (2008). doi:10.2475/02.2008.02

47. A. Blais-Stevens, J. J. Clague, Paleoseismic signature in late holocene sediment cores from Saanich Inlet, British Columbia. *Mar. Geol.* **175**, 131–148 (2001). doi:10.1016/S0025-3227(01)00132-3

48. W. Dyck, J. A. Lowdon, J. G. Fyles, W. Blake, Geological Survey of Canada radiocarbon dates V. *Radiocarbon* **8**, 96–127 (1966). doi:10.1017/S0033822200000072

49. N. F. Alley, Middle Wisconsin stratigraphy and climatic reconstruction, southern Vancouver Island, British Columbia. *Quat. Res.* **11**, 213–237 (1979). doi:10.1016/0033-5894(79)90005-X

50. G. Osborn, B. Menounos, C. Ryane, J. Riedel, J. J. Clague, J. Koch, D. Clark, K. Scott, P. T. Davis, Latest Pleistocene and Holocene glacier fluctuations on Mount Baker, Washington. *Quat. Sci. Rev.* **49**, 33–51 (2012). doi:10.1016/j.quascirev.2012.06.004

51. J. J. Clague, R. W. Mathewes, J. P. Guilbault, I. Hutchinson, D. P. Ricketts, Pre-Younger Dryas resurgence of the southwestern margin of the Cordilleran ice sheet, British Columbia, Canada. *Boreas* **26**, 261–278 (2008). doi:10.1111/j.1502-3885.1997.tb00855.x

52. J. A. Lowdon, W. Blake, Geological Survey of Canada Radiocarbon Dates XVIII. *Geol. Surv. Can. Pap.*, 1–20, Ottawa (1979).

53. W. Blake, Geological Survey of Canada Radiocarbon Dates XXIII. *Geol. Surv. Can. Pap.*, 12–23, Ottawa (1983).

54. I. R. Saunders, J. J. Clague, M. C. Roberts, Deglaciation of Chilliwack River valley, British Columbia. *Can. J. Earth Sci.* **24**, 915–923 (1987). doi:10.1139/e87-089

55. J. A. Lowdon, I. M. Robertson, W. Blake Jr., Geological survey of Canada radiocarbon dates XVII. *Geol. Surv. Can. Pap.* 77-7, Ottawa (1977).

56. J. A. Lowdon, W. Blake, Geological Survey of Canada Radiocarbon Dates IX. *Radiocarbon* **12**, 46–86 (1970). doi:10.1017/S0033822200036213

57. W. Dyck, J. G. Fyles, Geological Survey of Canada Radiocarbon Dates I. *Radiocarbon*. **4**, 13–26, Ottawa (1962).

58. J. E. Armstrong, Post-Vashon Wisconsin Glaciation, Fraser lowland, British Columbia. *Geol. Surv. Can. Bull.* **322**, 34 (1981).

59. A. Walton, M. A. Trautman, J. P. Friend, Isotopes, Inc. radiocarbon measurements, [Part] 1. *Radiocarbon* **3**, 47–59 (1961). doi:10.1017/S003382220002083X

60. G. R. Brooks, P. A. Friele, Bracketing ages for the formation of the Ring Creek lava flow, Mount Garibaldi volcanic field, southwestern British Columbia. *Can. J. Earth Sci.* **29**, 2425–2428 (1992). doi:10.1139/e92-190

61. J. A. Lowdon, W. Blake, Geological survey of Canada radiocarbon dates XVI. *Geol. Surv. Can. Pap.*, 76–77, Ottawa (1976).

62. J. A. Lowdon, W. Blake, Geological Survey of Canada Radiocarbon Dates XV. *Geol. Surv. Can. Pap.* **75–7**, 1–37, Ottawa (1975).

63. M. Margold, A. P. Stroeven, J. J. Clague, J. Heyman, Timing of terminal Pleistocene deglaciation at high elevations in southern and central British Columbia constrained by

^{10}Be exposure dating. *Quat. Sci. Rev.* **99**, 193–202 (2014). doi:10.1016/j.quascirev.2014.06.027

64. R. Minkus, thesis, University of Calgary (2006).

65. B. J. Mood, D. J. Smith, Latest Pleistocene and Holocene behaviour of Franklin Glacier, Mt. Waddington area, British Columbia Coast Mountains, Canada. *Holocene* **25**, 784–794 (2015). doi:10.1177/0959683615569321

66. J. A. Lowdon, I. M. Robertson, W. Blake, Geological Survey of Canada Radiocarbon Dates XI. *Radiocarbon* **13**, 255–324 (1971). doi:10.1017/S0033822200008456

67. M. Grubb, thesis, University of Northern British Columbia (2006).

68. J. A. Lowdon, W. Blake, Geological survey of Canada Radiocarbon Dates XIII. *Geol. Surv. Can. Pap.*, 73–77, Ottawa (1973).

69. A. Plouffe, V. M. Levson, Late Quaternary glacial and interglacial environments of the Nechako River - Cheslatta Lake area, central British Columbia. *Can. J. Earth Sci.* **38**, 719–731 (2001). doi:10.1139/e00-111

70. J. A. Lowdon, W. Blake, Geological survey of Canada radiocarbon dates XX Geol. Surv. Can. Pap., 80e87. *Geol. Surv. Can. Pap.*, 80–87, Ottawa (1980).

71. J. A. Lowdon, J. G. Fyles, W. Blake, Geological survey of Canada radiocarbon dates VI. *Radiocarbon* **9**, 156–197 (1967). doi:10.1017/S0033822200000503

72. W. Blake, Geological survey of Canada radiocarbon dates XXV. *Geol. Surv. Canada Pap.*, 85–87, Ottawa (1986).

73. N. Catto, D. G. E. Liverman, P. T. Bobrowsky, N. Rutter, Laurentide, cordilleran, and montane glaciation in the western Peace River–Grande Prairie region, Alberta and British Columbia, Canada. *Quat. Int.* **32**, 21–32 (1996). doi:10.1016/1040-6182(95)00061-5

74. J. M. Bednarski, I. R. Smith, Laurentide and montane glaciation along the Rocky Mountain Foothills of northeastern British Columbia. *Can. J. Earth Sci.* **44**, 445–457 (2007). doi:10.1139/e06-095

75. A. P. Stroeven, D. Fabel, M. Margold, J. J. Clague, S. Xu, Investigating absolute chronologies of glacial advances in the NW sector of the Cordilleran Ice Sheet with terrestrial in situ cosmogenic nuclides. *Quat. Sci. Rev.* **92**, 429–443 (2014). doi:10.1016/j.quascirev.2013.09.026

76. J. J. Clague, B. Ward, Pleistocene Glaciation of British Columbia, in *Developments in Quaternary Science*, vol. 15, J. Ehlers, P. L. Gibbard, P. D. Hughes, Eds. (Elsevier, Amsterdam, 2011), pp. 563– 573.